THEORETICAL & APPLIED MECHANICS LETTERS **2**, 022006 (2012)

Vortex-induced vibration of pipes conveying fluid using the method of multiple scales

Huliang Dai, and Lin Wang[a)]
Department of Mechanics, Huazhong University of Science and Technology, Wuhan 430074, China and Hubei Key Laboratory for Engineering Structural Analysis and Safety Assessment, Wuhan 430074, China

(Received 7 January 2012; accepted 16 January 2012; published online 10 March 2012)

Abstract The nonlinear dynamics of supported pipes conveying fluid subjected to vortex-induced vibration is evaluated using the method of multiple scales. Frequency response portraits for different internal fluid velocities under lock-in conditions are obtained and the stability of steady-state responses is discussed. Results show that the internal fluid velocity has a prominent effect on the oscillation amplitude and that the steady-state responses incorporating unstable solutions in the lock-in region are also obtained. In addition, the effects of two kinds of fluctuating lift coefficients on the steady-state responses are compared with each other. [doi:10.1063/2.1202206]

Keywords pipes conveying fluid, vortex-induced vibration, lock-in, steady-state responses, fluctuating lift

Vortex-induced vibration (VIV) frequently occurs in the ocean engineering when pipes are subjected to lateral currents. Especially when the vortex-shedding frequency is close to the natural frequency of the pipe, lock-in response, namely, resonance may spring up, resulting in relatively large-amplitude oscillation and accelerating the fatigue and damage of the structures. Therefore, the problem of pipes undergoing VIV is one of the hot concerned topics due to its engineering significance and academic interests.[1,2]

Most of the early experimental and theoretical studies on VIV of pipes/cylinders are restricted only to pipes without internal fluid flow.[3–8] Khalak and Williamson[9] observed the hysteresis loop phenomenon of the vibration amplitude with increasing current velocity in their experiments and recognized this phenomenon as initial, upper and lower response branches. Chen et al.[10] constructed a mathematical model of cylinders subjected to VIV based on the unsteady flow theory. Under the assumption of a sinusoidal lift and drag force, Wang et al.[11] adopted the ARMA technique for the analysis of VIV. In recent years, several theoretical and experimental studies on the vibration characteristics of pipes with axial internal fluid flow subjected to VIV were reported by Guo et al.,[12,13] Keber and Wiecigroch[14] and Meng and Chen,[15] all of whom stated that there is a strong effect of internal fluid flow on the VIV responses.

Based on the method of multiple scales, this paper aims to explore the nonlinear responses of VIV of pipes with internal fluid flow and to investigate the stability of steady-state responses in lock-in conditions. The present study employs a single degree of freedom model to simulate the lift force induced by the lateral currents and establishes the nonlinear equation of motion of pipes conveying axial fluid subjected to VIV. Moreover, the effect of variable lift coefficient used in this work on the VIV is compared with that of constant fluctuating lift coefficient.[16]

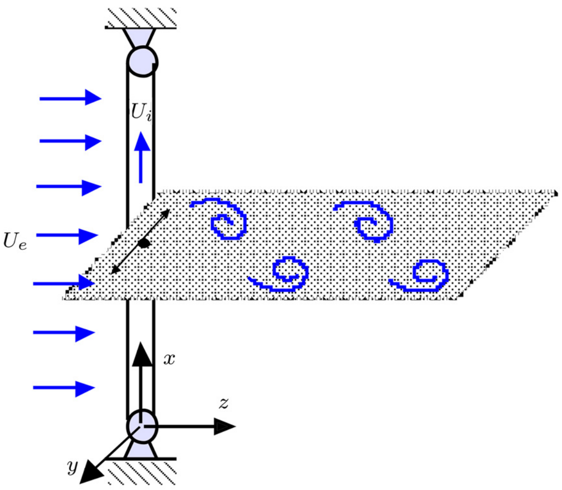

Fig. 1. Schematic of a simply supported pipe subjected to VIV.

The system under consideration consists of a slender pipe conveying internal axial fluid in a uniform cross-flow, as shown in Fig. 1. The pipe is simply supported at both ends. The pipe may move only in the direction normal to the external flow under the assumption that its flow-wise displacement is relatively small. If gravity, internal damping, externally imposed tension and pressurization effects are either absent or neglected, the equation under these conditions in cross-flow direction may take the following form

$$EI\frac{\partial^4 y(x,t)}{\partial x^4} + 2m_f U_i \frac{\partial^2 y(x,t)}{\partial x \partial t} + m_f U_i^2 \frac{\partial^2 y(x,t)}{\partial x^2} + m\frac{\partial^2 y(x,t)}{\partial t^2} - \frac{EA_p}{2L}\left[\int_0^L \left(\frac{\partial y(x,t)}{\partial x}\right)^2 \mathrm{d}x\right] \cdot$$

a) Corresponding author. Email: wanglindds@mail.hust.edu.cn.

$$\frac{\partial^2 y(x,t)}{\partial x^2} = f(x,t), \tag{1}$$

where $m = m_\mathrm{f} + m_\mathrm{p} + m_\mathrm{d}$, m_f, m_p and m_d are respectively defined as the mass per unit length of the internal fluid, the pipe and the added fluid, EI is the flexural rigidity of the pipe, A_p is the cross-section area of the pipe, L is the pipe length, U_i is the velocity of the internal flow, $f(x,t)$ represents the vortex-induced force acting on the pipe, $y(x,t)$ is the lateral displacement of the pipe, x and t are the axial coordinate and time, respectively. The force $f(x,t)$ may be given by[17]

$$\begin{aligned} f(x,t) &= f_\mathrm{D}(x,t) + f_\mathrm{L}(x,t) = \\ &-\frac{1}{2}C_\mathrm{D}\rho_o D U_\mathrm{e}\frac{\partial y(x,t)}{\partial t} + \\ &\frac{1}{2}\rho_o D U_\mathrm{e}^2 C_\mathrm{L}\cos(\omega_s t + \phi), \end{aligned} \tag{2}$$

where $f_D(x,t)$ is the drag force acting in the lateral direction, $f_L(x,t)$ is the lift force, U_e is the external flow velocity, ρ_o is the density of the external fluid, $C_D = 1.2$ is the drag coefficient in the transverse direction,[14] D is the outside diameter of the pipe; ω_s is the vortex-shedding frequency, ϕ indicates a phase angle. It should be pointed out that C_L is the fluctuating lift coefficient gained through curve-fitting. The experimental data of relationship between C_L and reduced steady amplitude was given by King.[16] By incorporating the following dimensionless quantities

$$\begin{aligned} &\tilde{y} = y/D, \quad \tilde{x} = x/L, \quad \beta = m_f/m, \\ &c = C_\mathrm{D}\rho_o D U_\mathrm{e} L^2/(2\sqrt{mEI}), \varOmega_s = \omega_s (m/EI)^{0.5} L^2, \\ &v = (m_f/EI)^{0.5} U_i L, \quad \alpha = \rho_o U_\mathrm{e}^2 L^4/(2EI), \\ &\gamma = A_p D^2/(2I), \tau = (EI/m)^{0.5} t/L^2, \end{aligned}$$

the equation of motion can be derived as

$$\begin{aligned} &\frac{\partial^2 \tilde{y}}{\partial \tau^2} + c\frac{\partial \tilde{y}}{\partial \tau} + 2\sqrt{\beta}v\frac{\partial^2 \tilde{y}}{\partial \tilde{x}\partial \tau} + \frac{\partial^4 \tilde{y}}{\partial \tilde{x}^4} + v^2\frac{\partial^2 \tilde{y}}{\partial \tilde{x}^2} - \\ &\quad \gamma\int_0^1 \left(\frac{\partial \tilde{y}}{\partial \tilde{x}}\right)^2 \mathrm{d}\tilde{x}\frac{\partial^2 \tilde{y}}{\partial \tilde{x}^2} = \alpha C_\mathrm{L}\cos(\varOmega_s \tau + \phi). \end{aligned} \tag{3}$$

As for Eq. (3), the Galerkin discretization may be used and the first order modal truncation with $\tilde{y} = \varPhi_1(\tilde{x})y_1(\tau)$ is adopted because of its main contribution. Then the ODE is obtained as follows

$$\ddot{y}_1 + \omega_1^2 y_1 = \gamma H_{11}R_{11}y_1^3 - c\dot{y}_1 + \tilde{\alpha}C_\mathrm{L}\cos(\varOmega_s\tau + \phi), \tag{4}$$

where

$$\begin{aligned} &\omega_1^2 = \int_0^1 \left[\varPhi_1^{(4)} + v^2\varPhi_1^{(2)}\right]\varPhi_1 \mathrm{d}\tilde{x}, \\ &H_{11} = \int_0^1 \varPhi_1^{(1)}\varPhi_1^{(1)}\mathrm{d}\tilde{x}, \quad R_{11} = \int_0^1 \varPhi_1^{(2)}\varPhi_1\mathrm{d}\tilde{x}, \\ &\tilde{\alpha} = 2\sqrt{2}\alpha/\pi, \end{aligned}$$

and $\varPhi_1$ is the eigenfunction of a simply supported beam. We scale y_1 with the factor $\varepsilon^{1/2}$ because of the smallness

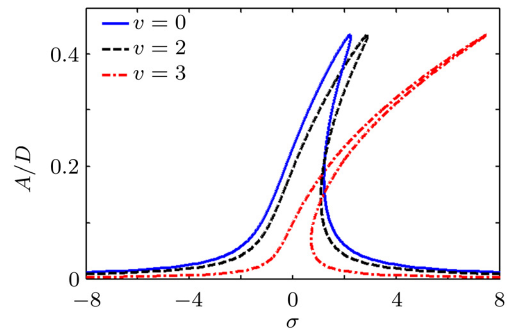

Fig. 2. Steady-state responses for different internal fluid velocities.

of the motion amplitude. As to the weak interaction between fluid and structure, we scale c and α with the factor ε. Thus,

$$\begin{aligned} \ddot{y}_1 + \omega_1^2 y_1 &= \varepsilon\gamma H_{11}R_{11}y_1^3 - \varepsilon c\dot{y}_1 + \\ &\varepsilon\tilde{\alpha}C_\mathrm{L}\cos(\varOmega_s\tau + \phi). \end{aligned} \tag{5}$$

To seek an approximate solution of Eq. (5), we introduce the time scale $T_n = \varepsilon^n\tau$, $n = 0, 1, 2, \ldots$. The time derivatives are

$$\begin{aligned} &\mathrm{d}/\mathrm{d}\tau = \partial/\partial T_0 + \varepsilon\partial/\partial T_1 + ..., \\ &\mathrm{d}^2/\mathrm{d}\tau^2 = \partial^2/\partial T_0^2 + 2\varepsilon\partial^2/(\partial T_0\partial T_1) + \ldots. \end{aligned} \tag{6}$$

We will focus on the dynamics of fluid-conveying pipes under lock-in conditions, i.e., $\varOmega_s = \omega_1 + \varepsilon\sigma$, where $\varOmega_s$ and ω_1 are respectively Strouhal frequency and the dimensionless natural frequency of the pipe, ε and σ are small perturbation parameter and detuning parameter, respectively. The expansion of y_1 is written in the form

$$y_1 = y_{10}(T_0, T_1) + \varepsilon y_{11}(T_0, T_1) + \ldots. \tag{7}$$

Substituting Eqs. (6) and (7) into Eq. (5) and equating coefficients of like powers of ε on both sides, one obtains

$$O(\varepsilon^0): \quad \frac{\partial^2 y_{10}}{\partial T_0^2} + \omega_1^2 y_{10} = 0 \tag{8}$$

$$\begin{aligned} O(\varepsilon^1): \quad &\frac{\partial^2 y_{11}}{\partial T_0^2} + \omega_1^2 y_{11} = -2\frac{\partial^2 y_{10}}{\partial T_0\partial T_1} + \\ &\gamma H_{11}R_{11}y_{10}^3 - c\frac{\partial y_{10}}{\partial T_0} + \\ &\tilde{\alpha}C_\mathrm{L}\cos(\varOmega_1 T_0 + \phi + \sigma T_1). \end{aligned} \tag{9}$$

The solution of Eq. (8) can be expressed as

$$y_{10} = A_1(T_1)\mathrm{e}^{\mathrm{i}\,\omega_1 T_0} + \bar{A}_1(T_1)\mathrm{e}^{-\mathrm{i}\,\omega_1 T_0}. \tag{10}$$

Substituting Eq. (10) into Eq. (9) and eliminating the secular terms, yields

$$\begin{aligned} &-2A_1'\mathrm{i}\omega_1 + \gamma H_{11}R_{11}3A_1^2\bar{A}_1 - cA_1\mathrm{i}\omega_1 + \\ &\tilde{\alpha}C_\mathrm{L}\frac{1}{2}\mathrm{e}^{\mathrm{i}\,(\phi + \sigma T_1)} = 0, \end{aligned} \tag{11}$$

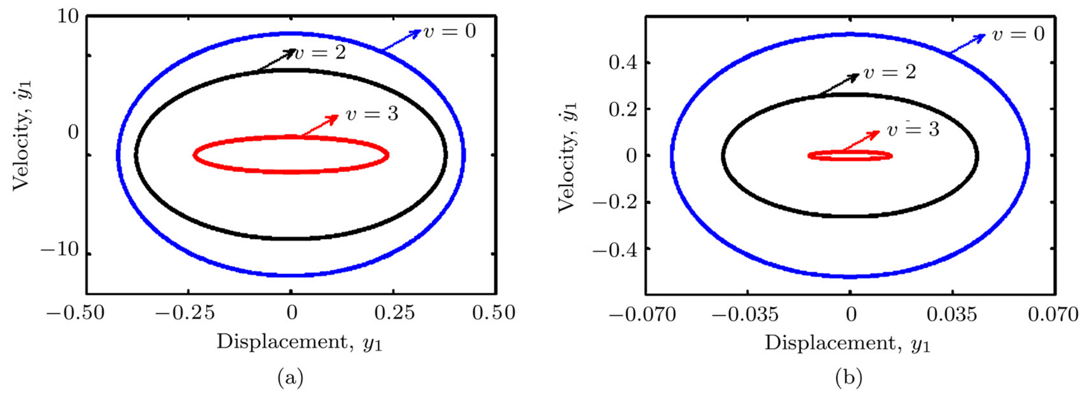

Fig. 3. Phase trajectories at upper branch (a) and lower branch (b) with $\sigma = 2$ for different internal fluid velocities.

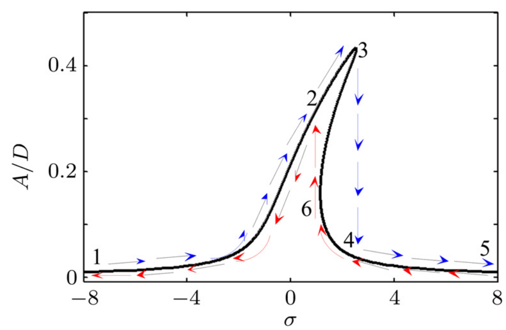

Fig. 4. A sample of frequency-response curve for $v = 1.5$.

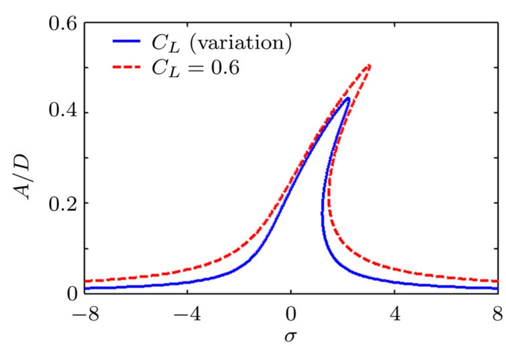

Fig. 5. Comparison between C_L varying with a_1 and $C_L = 0.6$ for $v = 0$.

where prime denotes differentiation with respect to the slow time T_1. Now introduce the polar transformation for the complex amplitude

$$A_1 = \frac{1}{2} a_1 \mathrm{e}^{\,\mathrm{i}\,\beta_1}, \tag{12}$$

where a_1 and β_1 are the real valued amplitude and phase, respectively. Substituting Eq. (12) into Eq. (11) and separating the real and imaginary parts, we get

$$a_1' = -\frac{1}{2} c a_1 + \frac{1}{2\omega_1} \tilde{\alpha} C_{\mathrm{L}} \sin\psi, \tag{13}$$

$$a_1 \psi' = a_1 \sigma + \frac{3}{8\omega_1} \gamma H_{11} R_{11} a_1^3 + \frac{1}{2\omega_1} \tilde{\alpha} C_{\mathrm{L}} \cos\psi, \tag{14}$$

where $\psi = \phi + \sigma \mathrm{T}_1 + \beta_1$. The steady-state solution of Eqs. (13) and (14) can be derived when

$$a_1' = 0, \quad \psi' = 0. \tag{15}$$

Through Eqs. (13)–(15), the frequency response equation can be derived

$$\left[\left(\frac{c}{2} \right)^2 + \left(\sigma + \frac{3\gamma H_{11} R_{11} a_1^2}{8\omega_1} \right)^2 \right] a_1^2 = \left(\frac{\tilde{\alpha} C_{\mathrm{L}}}{2\omega_1} \right)^2. \tag{16}$$

In the following calculations, the Young's modulus $E = 210$ GPa, the length $L = 150$ m, the outer diameter $D = 0.25$ m, the inner diameter $D_{\mathrm{i}} = 0.125$ m, the density of the pipe $\rho_{\mathrm{p}} = 7\,850$ kg/m^3, the density of the external fluid $\rho_o = 1\,020$ kg/m^3 and the density of the internal fluid $\rho_{\mathrm{i}} = 870$ kg/m^3. According to experimental data,[16] C_L can be simulated by a quartic polynomial: $C_L = -0.5a_1^4 + 2.4a_1^3 - 3.8a_1^2 + 1.9a_1 + 0.2$.

The steady-state responses at $x = 0.5L$ of the pipe for different internal fluid velocities are shown in Fig. 2. It is observed that the amplitude of the periodic motion decreases with increasing internal fluid velocity for a given σ, but that the maximum oscillating amplitude occurs as the vortex-shedding frequency is more deviating from the natural frequency of the pipe.

Figure 3 displays the sample phase portraits of upper and lower response branches for a given $\sigma = 2$. The phase portraits of the middle response branches cannot be obtained because of the instability of these steady-state solutions which will be discussed later.

A typical frequency response curve is depicted in Fig. 4 for a given internal flow velocity $v = 1.5$. For the sake of analyzing the jumping phenomenon, a small disturbance is assumed near the steady-state solution. Thus, we express

$$a_1 = a_0 + \hat{a}_1, \quad \psi = \psi_0 + \psi_1, \tag{17}$$

where a_0, ψ_0 are steady-state solutions, and $\hat{a}_1$, ψ_1 are small disturbances related to time. Therefore, C_L varies with a_0 in this case.

Substituting Eq. (17) into Eq. (16) and simplifying to linearization equations, one obtains

$$\begin{aligned}\hat{a}_1' &= -\frac{1}{2}c\hat{a}_1 + \frac{1}{2\omega_1}\tilde{\alpha}C_{\mathrm{L}}\cos\psi_0\psi_1,\\ \psi_1' &= \left(\frac{3}{4\omega_1}\gamma H_{11}R_{11}a_0 - \frac{1}{2\omega_1 a_0^2}\tilde{\alpha}C_{\mathrm{L}}\cos\psi_0\right)\hat{a}_1 - \\ &\quad \frac{1}{2\omega_1 a_0}\tilde{\alpha}C_{\mathrm{L}}\sin\psi_0\psi_1.\end{aligned} \tag{18}$$

Therefore, the stability of steady-state motion is determined by the eigenvalue λ of coefficient matrix in the right side of Eq. (18). Calculations show that the real part of eigenvalue λ is positive when a_0 is given between point 3 and 6, and that, however, when a_0 locates at other positions of the frequency response curve, the real part of eigenvalue λ is negative. Thus, the steady-state solutions between point 3 and 6 are unstable, and the phase portraits of the middle response branches cannot be obtained.

Another issue considered here is that whether the lift coefficient can be substituted by a constant, i.e. $C_L = 0.6$,[16] which is recognized by some researchers. It is shown in Fig. 5 that there are some differences whether from amplitude or from the lock-in region.

In conclusion, the effect of internal fluid velocity on VIV of pipes is explored based on a single degree of freedom model using the method of multiple scales. According to the results, vibration amplitude decreases with increasing internal fluid velocity in the lock-in condition. It is also shown that unstable steady-state responses exist in the lock-in regions. Furthermore, the fluctuating lift coefficient C_L may be given as a variation rather than a constant.

This work was partially supported by the National Natural Science Foundation of China (11172107) and the Program for New Century Excellent Talents in University (NCET-11-0183).

1. C. H. K. Williamson, and R. Govardhan, Journal of Wind Engineering and Industrial Aerodynamics **96**, 713 (2008).
2. X. D. Huang, H. Zhang, and X. S. Wang, Journal of marine sciences **27**, 95 (2009) (in Chinese).
3. D. Brika, and A. Laneville, Journal of fluid and Mechanics **250**, 481 (1993).
4. R. D. Gabbai, and H Benaroya, Journal of Sound and Vibration **282**, 575 (2005).
5. G. R. Franzini, and A. L. C. Fujarra, Journal of Fluids and Structures **25**, 742 (2009).
6. W. Chen, and Z. Zong, China offshore platform **25**, 26 (2010).
7. C. Norberg, Journal of Fluids and Structures **15**, 459 (2001).
8. Y. G. Tang, S. X. Zhang, and C. Yi, Journal of Sound and Vibration **297**, 408 (2006).
9. A Khalak, and C. H. K Williamson, Journal of Fluids and Structures **10**, 455 (1996).
10. S. S. Chen, S. Zhu, and Y. Cai, Journal of Sound and Vibration **184**, 73 (1995).
11. X. Q. Wang, R. M. C. So, and K. T. Chan, Journal of Sound and Vibration **260**, 287 (2003).
12. H. Y Guo, M. Lou, and X. L. Dong, et al, China Ocean Engineering **20**, 373 (2006)
13. H. Y. Guo, and M. Lou, Journal of Fluids and Structures **24**, 496 (2008).
14. M. Keber, and M. Wiercigroch, Journal of Sound and Vibration **315**, 685 (2008).
15. D. Meng, and L. Chen, Applied Ocean Research (2011) doi:10. 1016/j. apor. 2011. 10. 002.
16. S. S. Chen, *Flow-induced Vibration of Circular Cylindrical Structures* (Hemisphere Publishing Corp, Washington DC, 1987).
17. M P. Païdoussis, S. J. Price and E de Langre, *Fluid-Structure Interactions* (Cambridge University Press, Cambridge, 2011).